Quaternary International 445 (2017) 50–59

Contents lists available at ScienceDirect

Quaternary International

journal homepage: www.elsevier.com/locate/quaint

On the hindfoot bones of *Mammuthus trogontherii* from Shanshenmiaozui in Nihewan Basin, China

Xi Chen [a, b], Hao-wen Tong [a, *]

[a] Key Laboratory of Vertebrate Evolution and Human Origins of Chinese Academy of Sciences, Institute of Vertebrate Paleontology and Paleoanthropology, Chinese Academy of Sciences, Beijing 100044, China
[b] University of Chinese Academy of Sciences, Beijing 100049, China

ARTICLE INFO

Article history:
Available online 22 September 2016

Keywords:
Hindfoot bones
Mammuthus trogontherii
Ontogeny
Shanshenmiaozui
Nihewan
Early Pleistocene

ABSTRACT

Shanshenmiaozui is an open-air fossil site of Early Pleistocene age in Nihewan Basin, China. During 2006–2011, nearly 100 fossil specimens of *Mammuthus trogontherii* were unearthed, including some series of tarsal, metatarsal and phalange bones of immature individuals, which represent the first discovery of hindfoot bones of immature *M. trogontherii*. Morphologically, the new tarsals are intermediate between those of *Mammuthus meridionalis* and *Mammuthus primigenius*. However, they have some possible differences from those of *Palaeoloxodon antiquus*: the relatively quadrangled plantar surface of the astragalus; the relatively flat cuboid facet on calcaneum; and the special configuration of the distal facets on ectocuneiform. With reference to the age determination by teeth, the footbone remains can be categorized into three age groups: newborn calf, juvenile, and subadult, approximately corresponding to one month old, 6–7 years old, and 10–20 years old individuals, respectively. The ontogenetic changes of the hindfoot bones can be detected in their size, morphology, compact layer, and epiphyseal fusion. There are possibilities of proximal epiphyses on metatarsals and distal epiphyses on phalanges, which is unusual in other mammals, but reasonable in elephants because of their lengthy growth period.

1. Introduction

In the evolution of mammoth lineage, *Mammuthus trogontherii* is an intermediate species between the *Mammuthus meridionalis* and *Mammuthus primigenius* (Lister, 1993, 1996; Lister et al., 2005). The Nihewan Basin, which is located in the upland bordering the North China Plain, has attracted special attention for the origin of *M. trogontherii* (Wei et al., 2010). In Nihewan Basin the fossils from Majuangou site represent the earliest record of *M. trogontherii* in the world, dated back to 1.66 Ma (Wei et al., 2003; Zhu et al., 2004). During 2006–2011, the excavations at the Shanshenmiaozui site provided more abundant material of *M. trogontherii*, especially specimens of calf individuals (Tong, 2012; Tong and Chen, 2016). In 2011 some immature hindfoot bones which had never been found in the world were unearthed from Shanshenmiaozui. They could be attributed to the *M. trogontherii* as the only identified elephant in Shanshenmiaozui. In this paper we describe these rare hindfoot bones and investigate their morphological and ontogenetic significance.

The Shanshenmiaozui site lies at the core area of Nihewan Basin, surrounded by a series of Early Paleolithic sites (Hou and Zhao, 2010; Keates, 2010; Dennell, 2013). The fossils were unearthed from a 1-m thick sand-silt bed (Tong et al., 2011), which belongs to the fluvio-lacustrine sedimentary sequence of Nihewan Bed. The paleomagnetic age of the fossil layer is 1.2 Ma (Liu et al., 2016). The mammalian fauna includes *Lepus* sp., *Ochotona* sp., *Canis chihliensis*, Felidae gen. et sp. indet., *Pachycrocuta* sp., *M. trogontherii*, *Coelodonta nihowanensis*, *Elasmotherium peii*, *Proboscidipparion* sp., *Equus sanmeniensis*, *Sus* sp., *Eucladoceros* sp., *Spirocerus wongi*, *Gazella sinensis* and *Bison palaeosinensis* (Tong et al., 2011).

* Corresponding author.
E-mail address: tonghaowen@ivpp.ac.cn (H.-w. Tong).

http://dx.doi.org/10.1016/j.quaint.2016.09.001
1040-6182/

2. Methods and abbreviations

2.1. Methods

The measurements follow the methods described by Göhlich (1998), Von den Driesch (1976), and Ziegler (2001). The measurements of the bones were taken with sliding calipers or measuring box and are given in millimeters. “Breadth” stands for the mediolateral diameter; “length” stands for the proximodistal diameter; and “depth” stands for the dorsoplantar diameter. The CT image was taken with the 225 kV micro-computerized tomography of IVPP.

The ontogenetic stages follow the age categorizations provided by Sikes (1971) for *L. africana*, which includes the following age groups: calf (0–5 years old), juvenile (5–10 years old), subadult (10–20 years old), prime adult (20–40 years old), and senior adult (>40 years old).

2.2. Abbreviations

CKT: Chou-kou-tien (=Zhoukoudian) locality, China; **DEX:** dexter (right); **IVPP:** Institute of Vertebrate Paleontology and Paleoanthropology; **KIZ: Kunming Institute of Zoology; Loc:** locality; **Mt:** metatarsal; **SIN:** sinister (left); **SSMZ:** Shanshenmiaozui Locality; **V:** Catalog-Number-Prefix in IVPP.

3. Systematic paleontology

Class Mammalia Linnaeus, 1758
Order Proboscidea Illiger, 1811
Suborder Elephantiformes Tassy, 1988
Superfamily Elephantoidea Gray, 1821
Family Elephantidae Gray, 1821
Genus *Mammuthus* Brookes, 1828
***Mammuthus trogontherii* (Pohlig, 1885)**

3.1. Studied material

A total of 24 foot bones are included in this study (Table 1). These bones can be classified to 3 size-groups. The bones of each size-group are scattered in a particular square inside the excavation area, but most of the elements could match with one another when brought together. Based on their size and morphology, we correlate these 3 size-groups with the newborn calf, juvenile and subadult age groups, respectively.

Table 1
Fossil material of *M. trogontherii* studied in this paper.

Specimen	Field number	Catalog number	Square and horizon	Side	Ontogenetic stage
Astragalus	N-11-107	V18010.26	G21-8	Sin	II
Astragalus	N-11-171-c	V18010.27	H20-9	Dex	III
Astragalus	N-11-134-1	V18010.28	G24-8	Sin	III
Calcaneum	N-11-216	V18010.29	H20-9	Dex	I
Calcaneum	N-11-094	V18010.30	F20-8	Sin	II
Calcaneum	N-11-171-d	V18010.31	H20-9	Dex	III
Calcaneum	N-06-235	V18010.32	D11-6	Dex	III
Calcaneum	N-11-134-2	V18010.33	G24-8	Sin	III
Navicular	N-11-258	V18010.34	H20-10	Dex	I
Navicular	N-11-226	V18010.35	H21-9	Sin	II
Navicular	N-11-171-a	V18010.36	H20-9	Dex	III
Entocuneiform	N-11-219-3	V18010.37	H20-9	Dex	III
Mesocuneiform	N-11-219-2	V18010.38	H20-9	Dex	III
Ectocuneiform	N-11-219-1	V18010.39	H20-9	Dex	III
Cuboid	N-11-171-b	V18010.40	H20-9	Dex	III
Mt II	N-11-233	V18010.41	H20-10	Sin	I
Mt II	N-11-117	V18010.42	G21-8	Dex	II
Mt III	N-11-217	V18010.43	H20-9	Sin	I
Mt III	N-11-109	V18010.44	F21-8	Dex	II
Mt III	N-11-173	V18010.45	H20-9	Sin	III
Mt IV	H20-9-b	V18010.46	H20-9	Sin	I
Mt IV	N-11-198;	V18010.47	G21-9	Dex	II
Phalanx	n-11-274	V18010.48	H22-9	Sin?	I
Phalanx	n-11-145	V18010.49	H22-8	Dex?	II

3.2. Compared materials

Comparative data are from the following sources: *M. trogontherii* from such sites as Untermassfeld (Dubrovo, 2001), West Runton (Lister and Stuart, 2010), Loussika (Athanassiou, 2012), Azovland AzovII(Baygusheva et al., 2012) and Kostolac (Lister et al., 2012); *M. meridionalis* from Leu (Popescu, 2011) and Rodionovo (Maschenko et al., 2011); *M. primigenius* from Rottweil (Ziegler, 2001); *Palaeoloxodon antiquus* from Upnor (Andrews and Cooper, 1928) and CKT Loc.9 (Teilhard de Chardin, 1936); *Elephas maximus*: KIZ-1, 20–30 h old and KIZ-2, 2–3 years old.

3.3. Locality

Shanshenmiaozui, Yangyuan, Hebei, China.

3.4. Horizon

Lower Pleistocene, around 1.2 Ma.

The strata are consisted of the eolian loess and fluvio-lacustrine Nihewan Bed, with a thickness of 72 m. The fossiliferous layer is 1-m thick sand-silt bed, near to the bottom of Nihewan Bed.

3.5. Descriptions

3.5.1. Astragalus

No: V18010.26, juvenile (Fig. 1A; Table 2). This bone is perfectly preserved. Despite the neck and sulcus, the surface is full of

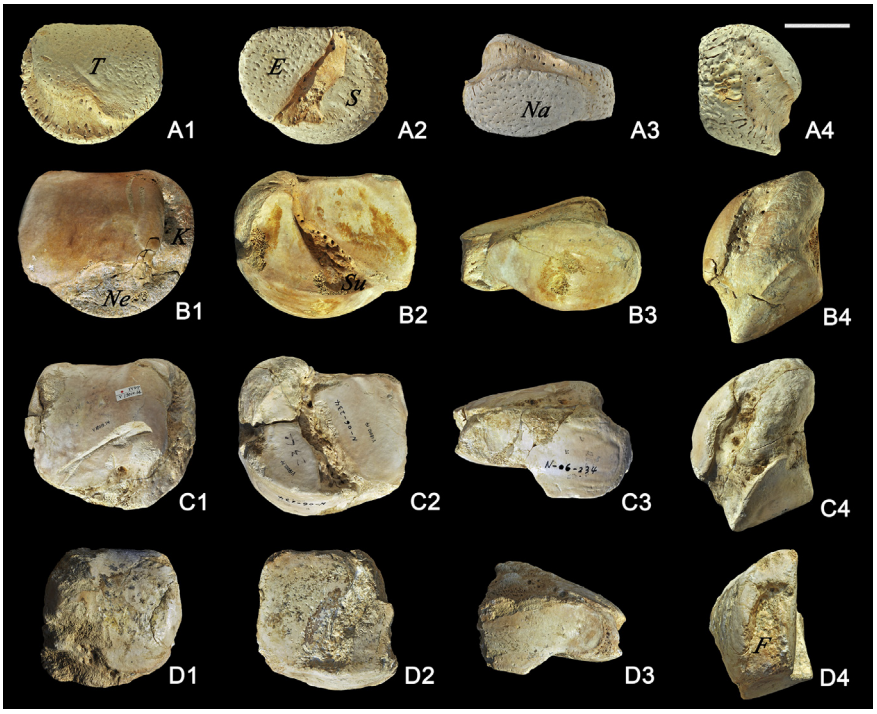

Fig. 1. Astragali of *M. trogontherii* from SSMZ in Nihewan Basin. A1–4: V18010.26; B1–4: V18010.27; C1–4: V18010.14; D1–4: V18010.28. A1–D1: dorsal view; A2–D2: plantar view; A3–D3: distal view; A4–C4: medial view; D4: lateral view. Scale bar equals 5 cm. **Abbreviation**: E: ectal facet; F: fibular facet; K: knob; Na: navicular facet; Ne: neck; S: sustentacular facet; T: tibial facet.

Table 2
Measurements of astragali of *M. trogontherii* from SSMZ, compared with those of related taxa.

Taxon	*M. trogontherii*								*M. Meridionalis*		*M.primigenius*
Site	This paper				West runton	Azovll	Loussika	Untermassfeld	Leu	Rodionovo	Rottweil
	V18010.26	V18010.27	V18010.14	V18010.28							
GB	110	130	127	101+	207	186	177	208	176	199	143
GL	91	117	114	106+	179	160	(150)	(188)	174	164	119
GDm	67	79	81	72+		110	90		102	119	88
Bt	93	108	104	103+	150	147				162	115
Ltm	71	90	93	–							
Ltl	82	96	97	99						146	97
Bcf	98	118	111+	–		158					131
Bsf	36	49	45+	–				(60)		54	
Lsf	63	72	77	84				134		110	82
Bef	67	84	67	65				106		89	
Lef	66	79	83	88				147		126	
Bnf	88	112	109	84+		162		150			116
Dnf	52	67	59	52+		85		87			62

Abbreviations: GB: Greatest breadth; GL: Greatest length: GDm: Greatest depth medial; Bt: Breadth of the trochlea; Ltm: Length of the trochlea medial; Ltl: Length of the trochlea lateral; Bcf: Breadth of the facet for calcaneum; Bsf: Breadth of the sustentacular facet; Lsf: Length of the sustentacular facet; Bef: Breadth of the ectal facet; Lef: Length of the ectal facet; Bnf: Breadth of the navicular facet; Dnf: Depth of the navicular facet.

numerous nutrient foramina and fissures, which are silted by the spongy, offwhite compacta.

Overall, this bone is broad and compact. In dorsal view the trochlea for the tibia is a roundish rectangle in outline, whereas its distolateral angle extends more forward. Below the trochlea, the neck and knob constitute a semi-circle on the distal and medial sides. The neck, which carries the navicular facet, is absent on the lateral side. On the medial side the knob is not as pronounced as in adults, and the fossa for ligament insertion has not formed yet. In plantar view the sustentacular facet is roughly semicircular in outline and the ectal facet is a roundish triangle with a rather straight inner edge. Both of these two facets are fairly flat. The sulcus is hollow in its center, where the floor is a bit rough. Two series of nutrient foramina lie along the walls of the sulcus. In distal view the navicular facet is convex and oval-shaped, making an angle of around 105° with the sustentacular one. In lateral view the facet for the fibula bears a shallow impression for ligament insertion.

No: V18010.27, subadult (Fig. 1B; Table 2). This bone is almost complete. It is well sculpted, and the compact layer has been formed well. In dorsal view the shape of the tibial trochlea is similar to the specimen V18010.26. On the medial side the knob

is quite pronounced, bears a remarkable fossa for ligament insertion, and extends much more proximally than the trochlea. In plantar view the sustentacular facet is semicircular, with an undulating surface; the ectal facet is an irregular triangle, with a relatively flat surface. The sulcus is widened distally and considerably rugged on the bottom. In distal view the navicular facet is oval in outline, making an angle with the sustentacular facet of ca. 120°. In lateral view the fibular facet forms an arc-shaped depression for ligament insertion.

No: V18010.14 (Fig. 1C) and V18010.28 (Fig. 1D; Table 2), subadult. V18010.14 is almost completely preserved; in V18010.28, the medial 1/4 of body is broken off. These two astragali are similar in shape. In dorsal view their knobs extend further proximally than in V18010.27. In plantar view the sustentacular facet is remarkably concave; the proximodistal diameters of the ectal facets are quite larger than the mediolateral ones, whereas it is opposite in V18010.27. In distal view the edge of the navicular facets forms a break angle on the distal border of the sulcus; on the contrary, this angle is roundish in V18010.26 and V18010.27. It is a possible trait of sexual dimorphism. The angle between the navicular and sustentacular facets is around 110°.

From juvenile to subadult, the astragalus shape is constant, despite the fact that the neck and knob are not pronounced in juveniles. Overall, the SSMZ astragali are similar to those of *M. meridionalis* from Leu (Popescu, 2011, pl. II), *M. trogontherii* from Loussika (Athanassiou, 2012, fig. 18e–f) and West Runton (Lister and Stuart, 2010, fig. 7). Even so, in the SSMZ specimens, the knob extends further proximally, making a distinct angle with the proximal border of the trochlea. Compared with *M. primigenius* from Steinheim (Dietrich, 1912, fig. 24), Rottweil (Ziegler, 2001, pl. 4) and Muirkirk (Harington et al., 2012, fig. 9), here the knob occupies less portion on the plantar surface. Compared with *P. antiquus*, the difference is significant. In our samples the neck does not extend to the lateral portion. Furthermore, the configuration of the sustentacular and ectal facets is nearly quadrangular in *M. trogontherii*, while it is subtrapezoid in *P. antiquus* (Andrews and Cooper, 1928, pl. VI). Generally, the SSMZ astragali are consistent with the mammoth type, but distinct from *P. antiquus*.

3.5.2. Calcaneus

No: V18010.29, newborn calf (Fig. 2A); and V18010.30, juvenile (Fig. 2B; Table 3). These two specimens are nearly complete. The compact layer is absent in V18010.29, since the surface is full of the nutrient foramina and fissures; in V18010.30, there is a layer of spongy, offwhite membrane, suggesting that the compact layer under formation. Morphologically, these two specimens are similar. Dorsally, the calcaneal tuber is quite short with a semi-circular contour on the lateroproximal side. The sustentacular facet is a roundish triangle at the lower level, while the ectal facet is nearly semi-circular in outline; on the distal border the sustentacular facet is much more backward than the ectal facet. In V18010.29 the sulcus between these two facets has two straight edges and gently widens distally; in V18010.30 the sulcus has undulating edges, greatly enlarged on the distal border, and markedly hollowed in middle course. On the plantar aspect, there is a faveolate, oval-shaped surface for epiphysis at the base of tuber. The body is constricted on the flank and rugged on the central area. In lateral view the fibular facet is indistinct, whereas it is partially visible on the lateroproximal side. Distally, the cuboid facet is quite flat on V18010.29, while it is markedly concave on V18010.30. The navicular facet cannot be detected.

No: V18010.31, subadult (Fig. 2C; Table 3). In this bone, the tuber is broken off, and the compact layer is fully mature. The

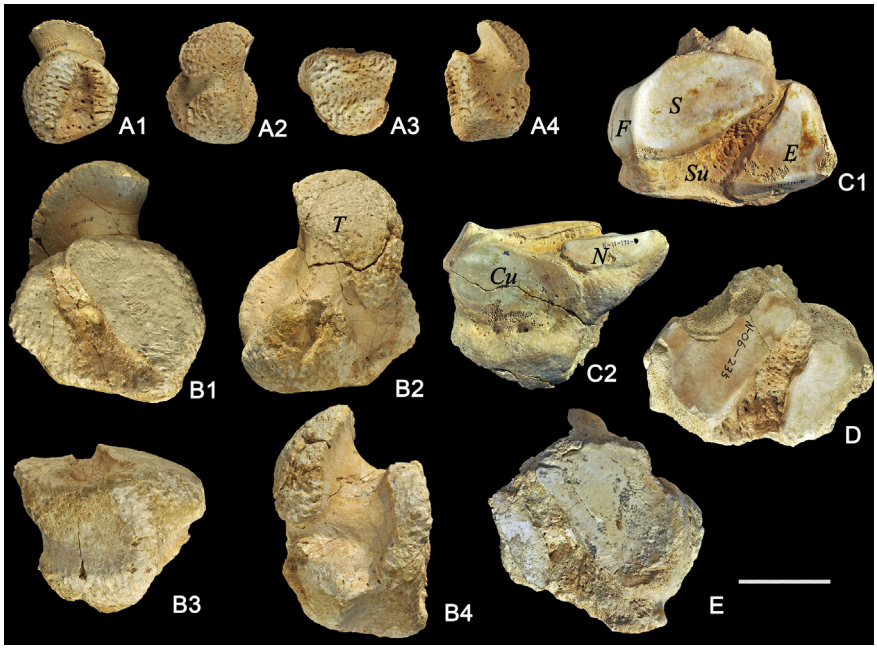

Fig. 2. Calcanea of *M. trogontherii* from SSMZ in Nihewan Basin. A1–4: V18010. 29; B1–4: V18010. 30; C1–2: V18010. 31; D: V18010. 32; E: V18010. 33. A1–C1, D, E: dorsal view; A2–B2: plantar view; A3–C3: distal view; A4–B4: medial view; D4: lateral view. Scale bar equals 5 cm. Abbreviation: Cu: cuboid facet; E: ectal facet; F: fibular facet; N: navicular facet; S: sustentacular facet; Su: sulcus; T: tuber.

Table 3
Measurements of calcanea of *M. trogontherii* from SSMZ, compared with those of related taxa.

Taxon	*M. trogontherii*									*M. Meridionalis*	*M. primigenius*	*P. antiquus*
Site	This paper				West runton	Azov II	Loussika	Untermassfeld	Kostolac	Leu	Rottweil	Upnor
	V18010.29	V18010.30	V18010.31	V18010.32								
GB	52	104	135	122+		(171)	197	213	195	178	141	218
GL	67	133	–	–	(205)	246	222	280	263	249	171	292
GD	45	81	104+	–			141	174	170.5	198		
Bct	37	84	–	–		167		145			81	111
Dct	47	86	–	–								174
Baf	(46)	(91)	117	112+							129	156
Laf	(49)	(82)	84								87	
Bsf	(18)	(29)	67	51+							47	
Lsf	(30)	(57)	58	58+				(125)			73	
Bef	(32)	(64)	86	78+				100			78	
Lef	(40)	(83)	70	63+				92+			73	
Bnf	–	–	56	–								
Dnf	–	–	19	–							38	
Bcf	–	–	80	–							76	
Dcf	–	–	53	–								

Abbreviations: GB: Greatest breadth; GL: Greatest length; GD: Greatest depth of calcaneal body; Bct: Breadth of the calcaneal tuber; Dct: Depth of the calcaneal tuber; Baf: Breadth of the astragalar face; Laf: Length of the astragalar face; Bsf: Breadth of the sustentacular facet for astragalus; Lsf: Length of the sustentacular facet for astragalus; Bef: Breadth of the ectal facet for astragalus; Lef: Length of the ectal facet for astragalus; Bnf: Breadth of the navicular facet; Dnf: Depth of the navicular facet; Bcf: Breadth of the cuboid facet; Dcf: Depth of the cuboid facet.

shape is relatively different from V18010.29 and V18010.30. In dorsal view the face for the astragalus is elongated in mediolateral direction. The sustentacular facet is almost a rectangular triangle beneath the kidney-shaped ectal facet. The distal border of the sustentacular facet exceeds that of the ectal facet. Both of these two facets are slightly undulating. On the sulcus, the bottom is gently hollow and rugged, with two rows of nutrient foramina along the walls. In plantar view the body is greatly contracted, bearing a number of permanent foramina. In lateral view the fibular facet is sector-shaped and tapers proximally. The angle between the fibular facet and the ectal facet is ca. 120°. In distal view the cuboid facet is oval-shaped and gently undulating. The navicular facet is small, semi-lunar in contour, adjacent to the sustentacular facet.

No: V18010.32 and V18010.33, subadults (Fig. 2D and E; Table 3). Only the dorsal parts are preserved. They are consistent in shape. The sustentacular facet is markedly inclined at the medioproximal angle, whereas the ectal facet rises laterally. The sulcus is very rough, bearing some well-opened foramina, and one can see a quite depressed pit in the middle of its course.

Fig. 3. Tarsals of *M. trogontherii* from SSMZ in Nihewan Basin. A1–3: navicular (V18010. 34); B1–3: navicular (V18010. 35); C1–3: navicular (V18010. 36); D: entocuneiform (V18010. 37); E1–3: mesocuneiform (V18010. 38); F1–4: ectocuneiform (V18010. 39); G1–2: cuboid (V18010. 40). A1–C1, E2–F2, G1: proximal views; A2–C2, D, E3–F3, G2: distal views; E1–F1: dorsal views; A3–C3: plantar views; G3: medial views; F4: lateral views. Scale bar is 2.5 cm for A1–3, while 5 cm for the rest. Abbreviations: A: astragalus facet; C: calcaneal facet; Cu: cuboid facet; Ec: ectocuneiform facet; En: entocuneiform; M: mesocuneiform; I: Mt I; II: Mt II; III: Mt III; IV: Mt IV; V: Mt V.

Overall, the calcanea of newborn calves and juveniles mostly resemble those of the Leu *M. meridionalis* (Popescu, 2011, photos 1–3) and the Loussika *M. trogontherii* (Athanassiou, 2012, fig. 18), as their sustentacular facets are much more backward than the ectal facets, and the cuboid facets are markedly skew with the navicular facets on distal border. However, the subadult specimens are similar to those of *M. primigenius* from Steinheim (Dietrich, 1912, fig. 26), Upnor (Andrews and Cooper, 1928, pl. VII), Rottweil (Ziegler, 2001, pl. 4), and Muirkirk (Harington et al., 2012, fig. 9). In V18010.31, the sustentacular facet is more forward than the ectal facet, thus the cuboid and navicular facets are nearly aligned. Here the ontogeny appearance notably coincides with the phylogeny relationship in mammoth lineage (Lister et al., 2005). Compared with the *P. antiquus* and *Loxodonta africana* (Andrews and Cooper, 1928, pl. VII), our specimens have a much more circular proximal margin of the tuber, and rather more flat cuboid facet.

3.5.3. Navicular

No: V18010.34, newborn calf (Fig. 3A); No: V18010.35, juvenile (Fig. 3B); No: V18010.36, subadult (Fig. 3C; Table 4). These three bones are nearly complete. The surface is full of nutrient foramina and fissures in newborn calf, covered by a layer of coarse compacta in juvenile, and finally wrapped by the mature compact layer in subadult. This bone is greatly compressed in proximodistal direction, with an oval to tongue-shaped outline. The proximal surface for the astragalus is mildly concave, while the distal surface is markedly convex. This convexity increases from newborn calf to subadult. Distally, there are three facets for tarsals: the outer facet is for the cuboid; the middle facet is for the ectocuneiform; and the inner one is shared by entocuneiform and mesocuneiform. Plantarly, the calcaneal facet cannot be detected until the juvenile stage; in subadult, this facet has a nearly semicircular contour, making an angle of ca. 130° with the astragalar facet. Here, the calcaneal facet is more elongated than that of Upnor straight-tusked elephant in mediolateral direction, and do not form a distinct process (Andrews and Cooper, 1928, pl. VI).

Table 4
Measurements of naviculars of *M. trogontherii* from SSMZ.

Dimensions	GB	GL	GD	Baf	Daf	Bda	Dda	Bcf	Lcf
V18010.34	40+	9	30	(35)	(25)	37+	(27)		
V18010.35	81	24	58	(70)	(49)	(79)	(52)		
V18010.36	118	43	78	(100)	66	118	74	52+	(18)

Abbreviations: GB: Greatest breadth; GL: Greatest length; GD: Greatest depth; Baf: Breadth of the astragalar facet; Daf: Depth of the astragalar facet; Bda: Breadth of distal articulation; Dda: Depth of distal articulation; Bcf: Breadth of calcaneal facet; Lcf: Length of calcaneal facet.

3.5.4. Entocuneiform

No: V18010.37, subadult (Fig. 3D; Table 5). This bone is broken on its proximal and ventral sides. Distally, there is a slightly concave facet for the hallux, nearly triangular in outline. Laterally, the facet for the mesocuneiform is partly preserved, making an angle of ca. 125° with the distal surface.

Table 5
Measurements of entocuneiform of *M. trogontherii* from SSMZ.

Dimensions	GB	GL	GD
V18010.37	34+	21+	40+

3.5.5. Mesocuneiform

No: V18010.38, subadult (Fig. 3E; Table 6). This bone is almost complete, but slightly damaged on its plantar side. It is nearly a right triangle in shape and terminates into a knob in plantar direction. Proximally, the navicular facet is slightly concave, with a arc-shaped groove on its central area. Distally, the facet for the Mt IIis rather flat. Medially, the facet for the entocuneiform is semicircular in outline. Laterally, there are two strip-like facets for the ectocuneiform, with a ditch between them. This specimen differs remarkably from the mesocuneiform of Rottweil woolly mammoth, since the latter one is a vertically elongated obtuse triangle in outline (Ziegler, 2001, pl. 4).

Table 6
Measurements of mesocuneiform of *M. trogontherii* from SSMZ.

Dimensions	Bdo	GD	GL	Becf	Decf	Lecf	Decf	Bdf	Ddf	Dm	Dl
V18010.38	52	59	29	49	55	14	21+	53	(59)	56	74

Abbreviations: Bdo: Breadth dorsal; GD: Greatest depth; GL: Greatest length; Becf: Breadth of the facet for ectocuneiform; Decf: Depth of the facet for ectocuneiform; Lecf: Length of the facet for entocuneiform; Decf: Depth of the facet for entocuneiform; Bdf: Breadth of the distal facet for MtII; Ddf: Depth of the distal facet for MtII; Dm: Depth medial; Dl: Depth lateral.

3.5.6. Ectocuneiform

No: V18010.39, subadult (Fig. 3F; Table 7). It is completely preserved. The outline is nearly an isosceles triangle, bearing a knob on its plantar end. Proximally, it is gently concave in dorsoplantar direction. Distally, it is mildly convex, with a small narrow facet for the Mt II and a big triangular facet for the Mt III. These two facets make an angle of ca. 135°. In *P. antiquus*, *L. africana* and *Elephas maximus* the distal surface of the ectocuneiform is shared by the facets for the Mt III and Mt IV; the facet for the Mt IV forms a protuberance laterally (Andrews and Cooper, 1928, pl. VIII). Medially, there are two crescent-shaped facets articulated with the mesocuneiform; between them is a ditch with rugged surface. Laterally, the two facets for the cuboid are continuous. Generally, this bone is similar to those of *M. trogontherii* from Rottweil (Ziegler, 2001, pl. 4) and *M. meridionalis* from Leu (Popescu, 2011, photo 6).

Table 7
Measurements of ectocuneiform of *M. trogontherii* from SSMZ.

Dimensions	GB	GL	GD	Bcf	Dcf	Bdf	Ddf	Dm	Dl
V18010.39	56	37	93	47+	69+	49	89	(88)	97

Abbreviations: GB: Greatest breadth; GL: Greatest length; GD: Greatest depth; Bcf: Breadth of the facet for cuboid; Dcf: Depth of the facet for cuboid; Bdf: Breadth of the distal facet for Mt III; Ddf: Depth of the distal facet for Mt III; Dm: Depth medial; Dl: Depth lateral.

3.5.7. Cuboid

No: V18010.40, subadult (Fig. 3G; Table 8). This bone is intact. It is an almost equilaterally triangle in shape and mildly convex in proximodistal direction. Proximally, the navicular facet is roughly triangular, neighboring with an oval-shaped facet for the calcaneum which is slightly undulating. Distally, the facet for the Mt IV is nearly triangular in shape, while the facet for the Mt V is short and circular. These two facets are continuous. On its plantar end there is a bony knob which is partly separated from the metatarsal facets by a remarkable pit. In the pit one can see a big nutrient foramen. Medially, two facets for the ectocuneiform are located on the dorsodistal or proximoplantar side respectively; they are confluent at the center of the medial plane. Compared with the *P. antiquus* from Upnor (Andrews and Cooper, 1928, pl. VII), here the knob has not formed as a distinct tubercle. This difference can also be observed in *M. meridionalis* (Popescu, 2011, photo 5), *M. trogontherii* (Athanassiou, 2012, fig. 18) and *M. primigenius* (Ziegler, 2001, pl. 5). In general, the cuboids in the mammoth lineage are similar.

Table 8
Measurements of cuboid of *M. trogontherii* from SSMZ.

Dimensions	GB	GL	GD	Bcf	Dcf	Bnf	Dnf	Lpfe	Dpfe	Ldfe	Ddfe	Bda	Dda	Dm	Dl
V18010.40	91	41	88	40	(55)	33	(58)	11	23	(11)	28	85	68	97	90

Abbreviations: GB: Greatest breadth; GL: Greatest length; GD: Greatest depth; Bcf: Breadth of calcaneal facet; Dcf: Depth of calcaneal facet: Bnf: Breadth of navicular facet; Dnf: Depth of navicular facet; Lpfe: Length of the proximal facet for ectocuneiform; Dpfe: Depth of the proximal facet for ectocuneiform; Ldfe: Length of the distal facet for ectocuneiform; Ddfe: Depth of the distal facet for ectocuneiform; Bda: Breadth of distal articulation; Dda: Depth of distal articulation; Dm: Depth medial; Dl: Depth lateral.

3.5.8. Mt II

No: V18010.41, newborn calf (Fig. 4A); No: V18010.42, juvenile (Fig. 4D; Table 9). They are intact except for the unfused distal epiphyses. On the shaft the compact layer is nearly well formed; on the proximal epiphysis (metaphysis) the development of the compact layer is similar to that of the tarsals, as it is absent on V18010.41, then semi-fused on V18010.42. Both of these bones are short and stout, with a quadrangular cross-section. The dorsal and lateral sides are rather delimited, while the medial and plantar sides confluent to be a circular arc. On V18010.42 the concavity of the shaft is quite strong on dorsal and plantar aspects. Dorsally, the suture between the proximal epiphysis (metaphysis) and the shaft is ditch-like and bends forward on the medial side. Proximally, one can see a large facet for the mesocuneiform and a small facet for the ectocuneiform, however their contours are more defined in V18010.42. Distally, there is a faveolate surface for the epiphyseal plate. Medially, there is a small bump beneath the dorsal edge, which bears a facet for the entocuneiform. In front of this bump, there is a remarkable depression for musculature insertion. Laterally, a gently rugged depression for muscular insertion can be observed on proximal end; in V18010.42, there are several foramina in this depression.

Table 9
Measurements of metatarsals of *M. trogontherii* from SSMZ.

Dimensions		GL	Bp	Dp	SBd	SDd	Bdd	Ddd
Mt II	V18010.41	32	25	28	22	23	27	27
	V18010.42	53	40	47	31	29	38	41
	KIZ-1-1	34	17				18.5	
	KIZ-2-1	41					31	
Mt III	V18010.43	34	23	30	23	23	27	28
	V18010.44	61	40	51	33	33	45	44
	V18010.45		62	79				
	KIZ-1-2	37	20				22	
	KIZ-2-2	52					36	
Mt IV	V18010.46	31	29	25	25	23	29	27
	V18010.47	55	51	42	30	34	41	46
	KIZ-1-3	35	21				24	
	KIZ-2-3	46					41	

Abbreviations: GL: Greatest length; Bp: Breadth proximal; Dp: Depth proximal; SBd: Smallest breadth of the diaphysis; SDd: Smallest depth of the diaphysis; Bdd: Breadth of distal end of diaphysis; Ddd: Depth of distal end of diaphysis.

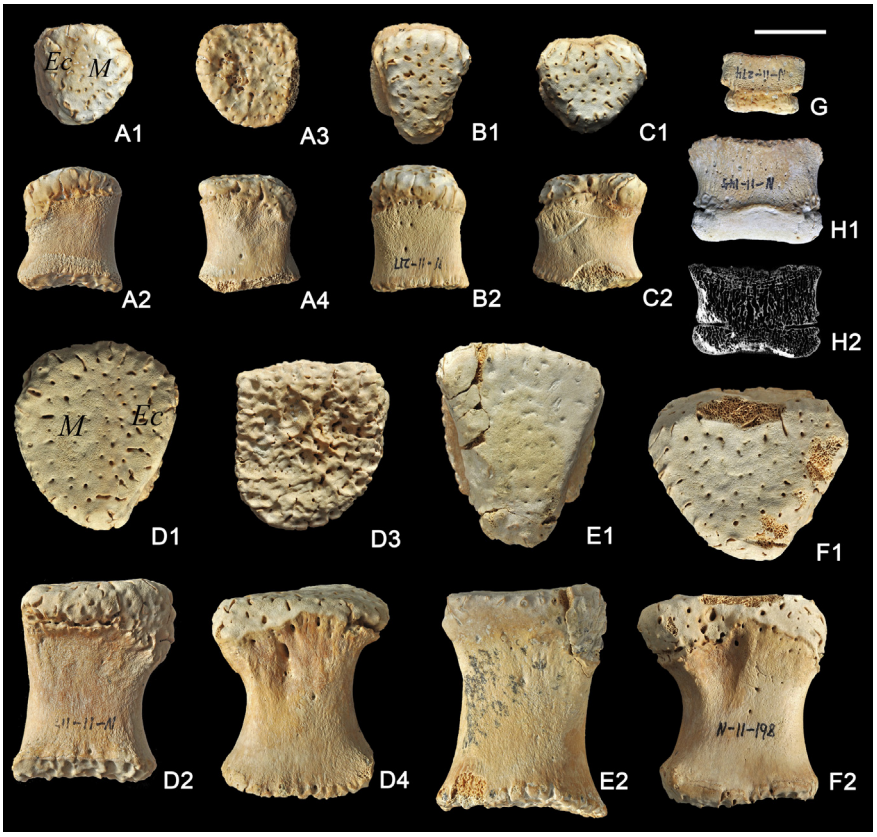

Fig. 4. Metatarsals and phalanges of *M. trogontherii* from SSMZ in Nihewan Basin. A1–4: Mt II (V18010. 41); B1–2: Mt III (V18010. 43); C1–2: Mt IV (V18010. 46); D1–4: Mt II (V18010. 42); E1–2: Mt III (V18010. 44); F1–2: Mt IV (V18010. 47); G: 1st phalanx of 3rd toe (V18010. 48); H1–2: 1st phalanx of 3rd toe (V18010. 49). A1–F1: proximal views; A2–F2, G, H1: dorsal views; A3, D3: distal views; A4, D4: lateral views; H2: CT image. Scale bar equals 2 cm. Abbreviations: Ec: ectocuneiform facet; M: mesocuneiform.

3.5.9. Mt III

No: V18010.43, newborn calf (Fig. 4B); No: V18010.44, juvenile (Fig. 4E; Table 9). These two bones are intact, except for their unfused distal epiphyses. On the shaft the compact layer has been formed well; on proximal epiphysis (metaphysis) the compact layer is absent in newborn calf, while semi-fused at juvenile stage. The Mt III is slender and more elongated than the Mt II and Mt IV. The proximal epiphysis (metaphysis) is semi-fused with the shaft where the suture is visible. In cross-section, the shaft is a laterally symmetric quadrangle, while it contracts plantarly. Proximally, one can see a facet for the ectocuneiform, which is an isosceles triangle in outline. Distally, the surface for epiphyseal plate is faveolate. On both dorsal and plantar sides, the specimen V18010.43 is mildly concave, while the concavity is quite stronger in specimen V18010.44. In the flank, the facets for neighboring metatarsals are vague in V18010.43, while quite distinct in V18010.44. There are several foramina in the pits for ligament insertion.

No: V18010.45, subadult. Only the proximal end is preserved. The compact layer has been well fused. The proximal surface is triangular and flat. Medially, one can see a dorsoplantarly elongated facet for the MtII, which extends to the plantar end. Laterally, the facets for the Mt IV are a bit shorter. The pits for ligament insertion are developed on the flank. There is a remarkable tuberosity near the proximoplantar end. The size of the proximal facet fits with that of the adult *M. primigenius*.

3.5.10. Mt IV

No: V18010.46, newborn calf (Fig. 4C); No: V18010.47, juvenile (Fig. 4F; Table 9). Except for the unfused distal epiphyses, these two bones are complete. On the shaft, the compact layer is well formed; whereas on the proximal epiphysis (metaphysis) the compact layer is absent in the newborn calf, but semi-fused at the juvenile stage. They are short and stout in shape. The proximal facet is triangular in outline, while the facet for the cuboid is flat. The dorsal surface of the shaft is a roundish quadrangle in shape, with a quite straight lateral margin. The shaft mildly contracts to the central part on specimen V18010.46, however, this contraction is much stronger on specimen V18010.47. In side view the facet for the Mt III cannot be detected, and the facet for the Mt V appears in the juvenile. Dorsally, there is a depression for musculature attachment in the proximal end.

3.5.11. Phalanges

No: V18010.48, newborn calf (Fig. 4G); No: V18010.49, juvenile (Fig. 4H; Table 10). These two bones are perfectly preserved, except for their unfused proximal epiphyses. They are hard to be assigned as fore or hind phalanges by shape, but probably belong to the hindfoot, together with the associated metatarsals; they are certainly the first phalanges, and most likely belong to the third toe because of their symmetrical appearance. On the distal epiphysis (metaphysis), the V18010.48 is full of nutrient foramina and fissures, because of the absence of compact layer. However, on V18010.49 the compact layer is a layer of spongy, offwhite membrane. On the whole, the phalanges are compressed dorsoplantarly. The distal epiphysis (metaphysis) is partly fused with the diaphysis, with two ditches on flank sides. From the CT image, one can see the distal epiphysis (metaphysis) only fused with the shaft on the central part (Fig. 4-H2). Proximally, there is an oval-shaped, faveolate surface for proximal epiphyseal plate. Distally, the facet for the middle phalange is slightly concave on its center. Dorsally, the surface inclines forward and the body is nearly symmetric. Plantarly, the concavity of the shaft is mildly in V18010.48, while it is remarkably concave in V18010.49 and bears several permanent foramina.

Table 10
Measurements of phalanges of *M. trogontherii* from SSMZ.

Dimensions	V18010.48	V18010.49
GL	15	27
Bp	22	37
Dp	19	29
Bd	20	36
Dd	12	21

Abbreviations: GL: Greatest length; Bp: Breadth of proximal end of diaphysis; Dp: Depth of proximal end of diaphysis; Bd: Breadth distal; Dd: Depth distal.

4. Discussion

4.1. Taxonomic assignment

Three kinds of elephantids have been reported from Early Pleistocene Nihewan Basin, including *M. meridionalis*, *M. trogontherii*, and *P. namadicus*. Since the first appearance of *Palaeoloxodon* is between 0.8 and 0.6 Ma in Eurasia, the specimens of SSMZ cannot be placed in genus *Palaeoloxodon* for its old geologic age. In Nihewan Basin the *M. meridionalis* and *M. trogontherii* have been dated to 2.6 Ma to 1.8 Ma and 1.66 Ma to 1.1 Ma respectively (Zhu et al., 2004; Wei et al., 2006). Even in East Asia, no *M. meridionalis* fossil record is later than 1.8 Ma (Wei et al., 2010). In morphology both dp2/DP2 and dp3/DP3 of SSMZ have at least one more plates than all the known *M. meridionalis* (Tong, 2012, Table 2/3; Tong and Chen, 2016, Table 3/4), with only one exception. Furthermore, the SSMZ fauna is kind of steppe fauna (Tong et al., 2011), representing the cool and dry environment. However, the *M. meridionalis* is generally acknowledged as an indicator of the Savana-like environment (Garutt, 1998; Baygusheva and Titov, 2012). Based on the biostratigraphy, dental morphology and palaeoenvironment evidence, the *M. trogontherii* is the only reasonable option for SSMZ materials.

On the tarsals, we also recognized some possible characters taxonomic value. The shapes of the astragali and calcanea are intermediate between those of *M. meridionalis* and *M. primigenius*, but distinct from *P. antiquus*. On the astragalus, the surface for the calcaneum is nearly quadrangular in *M. trogontherii*, while it is markedly irregular in *P. antiquus*. On the calcaneum, the cuboid facet is quite more flat than that of *P. antiquus*. On the navicular and cuboid, the facets for each other are rather more elongated in mediolateral direction. On the ectocuneiform, the distal surface is shared by the Mt II and Mt III in mammoth, whereas by Mt III and Mt IV in *P. antiquus*. However, since the comparing material is insufficient, these characters should be tested by more findings in the future.

4.2. Age estimation

The common method for age determination of mammoth is based on tooth eruption and wear (Haynes, 1991), which was firstly applied to the African elephant (*L. africana*), Asian elephant (*E. maximus*) (Laws, 1966; Roth and Shoshani, 1988). Of the postcranial skeleton, the fusion order of limb-bone epiphyses can also provide an approximate age determination, as the skeleton growth of mammoth can continue into adulthood (Lister, 1999). Nevertheless, it is hard to estimate the age of a mammoth merely on the foot bones.

In SSMZ, the hindfoot bones of the first ontogenetic stage are very tiny. The associated maxilla (V. 18010.15) and mandible (V. 18010.24) have been estimated to be one-month-old (Tong and Chen, 2016). Therefore, these hindfoot bones should belong to a one-month-old newborn calf. In the second ontogenetic stage, these bones are still beyond the maturity, because of the partial fused compact layer and markedly small size. Among them, the proximal epiphysis of the first phalanx of the third toe (V18010. 49)

has not been fused with the shaft, while this happens before the eighth year of life on the third finger of *E. maximus* (Siegal-Willott et al., 2008). Since the manual phalanges and pedal phalanges have almost the same ossification sequence in *L. africana* (Hautier et al., 2012), we consider that this individual is no more than 8 years old. Furthermore, the size of the astragalus (V18010.26) is close to that of the distal end of the tibia (PIN4353-625) at the 6–7 years old *M. primigenius* (Maschenko, 2002). Thus, perhaps this individual is around 6–7 years old. The specimens in the third ontogenetic stage represent two individuals. They have a mature appearance, but they are still significantly smaller than the known mature mammoths. Obviously, their tibial distal epiphyses were still under growth, when the animal died. The age of fusion between the epiphysis and diaphysis of the tibia is 27 years in the male woolly mammoth, and that should be much earlier on the female (Lister, 1999). Therefore, the specimens of the third ontogenetic stage are likely to belong to the 10–20 years old subadults.

4.3. Ontogeny

In living elephantids, the knowledge on the ontogeny of the postcranial skeleton is mainly from the results of X-ray or CT scanning (Miller et al., 2008; Siegal-Willott et al., 2008; Hautier et al., 2012). Concerning the woolly mammoth, both the mummies (Maschenko et al., 2013a,b; Fisher et al., 2014) and the calf bones (Maschenko, 2002, 2006; Maschenko et al., 2005) provide some meaningful information about the development of the teeth, limb bones and body size. Here, the SSMZ specimens provide an opportunity to investigate the ontogenetic significance of the hindfoot bones, including the shape, compact layer and the fusion of ossification centers.

From the newborn calf to the subadult, the relief for muscular insertion and the outline of the facets have been formed as expected. In the newborn calf, the metatarsals are short and stout. Then in juvenile, the shaft contracts on the middle part, showing markedly allometry between the ends and the shaft. The metatarsals also express relative reduction of the transverse diameters of their shafts in comparison with their lengths, as the limb bones of *M. primigenius* (Maschenko, 2002). The astragalus and calcaneum mostly resemble the *M. meridionalis* in newborn calf and juvenile, but are rather similar to the *M. primigenius* in subadult. It seems that this change agrees with the phylogeny of the mammoth lineage.

The fusion of the compact layer is associated with the reduction of additional foramina; the initial material is a matrix of spongy, offwhite membrane. On the tarsals, the compact layer is not formed at the newborn calf and juvenile stage. But for the metatarsals, the compact layer has been almost formed on the diaphysis during the newborn calf period. This is the same as the limb bones of *M. primigenius* (Maschenko, 2002). Apparently, both of the limb bones and metatarsals start the forming process of compact layer at the last prenatal stage, which is quite earlier than the tarsals. Perhaps this can be partly attributed to the relatively later ossification time of the tarsals (Hautier et al., 2012).

During the newborn calf and juvenile period, the hindfoot elements of *M. trogontherii* are also distinct for the fusion among the ossification centers. The calcaneus is the only tarsal that has two ossification centers. On either V18010.29 or V18010.30, there is an oval-shaped faveolate surface at the end of the calcaneal tuber. It suggests that the epiphysis has not been fused with the calcaneus in the juvenile. In our specimens the distal epiphyses of the metatarsals and the proximal epiphyses of the phalanges are missing, with the faveolate surface for the epiphyseal plates. In the proximal end of metatarsals and distal end of phalanges, the growth centers are very similar to the epiphyses, since they are separated from the diaphyses with distinct ditches and their surfaces are full of nutrient foramina. These 'opposite epiphyses' have been rarely reported before, except for the Mc/Mt I of human (Gray, 1918; Peterson, 2007). However Silver (1969) noted that the 'opposite epiphyses' exists in domestic animals and most of them have been fused to the diaphyses before birth. It is possibly that the metatarsals and phalanges have two epiphyses in both proximal and distal ends, like the limb bones. Since the elephant can continue growing into adult life and the epiphyses of limb bones fuse very late (Roth, 1984; Lister, 1999), it could be reasonable that these 'opposite epiphyes' of metatarsals and phalanges can still be detected at the juvenile stage. Even so, we can't definitely rule out the possibility of metaphyses, as the knowledge on the growth of foot bones is poor.

5. Conclusion

The hindfoot bones studied in this paper come from the Lower Pleistocene horizon of Nihewan Basin, belong mostly to immature elements and represent the first report on immature postcranial bones of *M. trogontherii*. The associated remains represent 4 individuals, ranging from the newborn calf, juvenile and subadult. Morphologically, the remains are between those of *M. meridionalis* and *M. primigenius*, but they differ from those of *Palaeoloxodon* in some degree. In combination with associated juvenile tooth material, the hindfoot bones should be referred to the species *M. trogontherii*. The ontogeny of the hindfoot elements reflects patterns of allometry on the shape and heterochrony on compact layer formation. Our research supports that elephants have a lagging process of epiphyseal fusion in contrast with other mammals, due to their lengthy growth period.

Acknowledgements

The authors are grateful to Han F., Xu Z.-J., Yin C., Hu N. and Wang X.-M. for assistance with the field work and Wei Q. for providing the site information. We also give heartfelt thanks to Dr. Li Q. for measuring the specimens in KIZ, to Professor Ni X.-J. for helpful discussions and to Dr. Larramendi for bibliographies. This work was supported by National Natural Science Foundation of China (Grant No: 41572003); Key Research Program of the Chinese Academy of Sciences (Grant No: KZZD-EW-15); the project from the P.R.C. Ministry of Land and Resources (Grant No: 201211005-3) and the Special Fund for Fossil Excavation and Preparation of the Chinese Academy of Sciences.

References

Andrews, C.W., Cooper, C.F., 1928. On a Specimen of *Elephas antiquus* from Upnor. British Museum (Natural History), London, pp. 1–26.
Athanassiou, A., 2012. A skeleton of *Mammuthus trogontherii* (Proboscidea, Elephantidae) from NW Peloponnese, Greece. Quaternary International 255, 9–28.
Baygusheva, V., Titov, V., 2012. The evolution of Eastern European meridionaloid elephants' dental characteristics. Quaternary International 255, 206–216.
Baygusheva, V.S., Titov, V.V., Timonina, G.I., 2012. Two skeletons of *Mammuthus trogontherii* from the Sea of Azov region. Quaternary International 276, 242–252.
Dennell, R.W., 2013. The Nihewan Basin of North China in the early Pleistocene: continuous and flourishing, or discontinuous, infrequent and ephemeral occupation? Quaternary International 295, 223–236.
Dietrich, W.O., 1912. Elephas primigenius Fraasi, eine schwäbische Mammutrasse. Jahreshefte des Vereins für Vaterländische Naturkunde in Württemberg 68, 42–106.
Dubrovo, I., 2001. Remains of Elephantidae from the lower Pleistocene site of Untermassfeld. Das Pleistozän von Untermaßfeld bei Meiningen (Thüringen), Teil 2, 589–605.
Fisher, D.C., Shirley, E.A., Whalen, C.D., Calamari, Z.T., Rountrey, A.N., Tikhonov, A.N., Buigues, B., Lacombat, F., Grigoriev, S., Lazarev, P.A., 2014. X-ray computed tomography of two mammoth calf mummies. Journal of Paleontology 88 (4), 664–675.

Garutt, W.E., 1998. Is there a genus Archidiskodon Pohlig, 1885, of the family Elephantidae Gray, 1821? Cranium 15 (1), 15–20.
Göhlich, U.B., 1998. Elephantoidea (Proboscidea, Mammalia) aus dem Mittel-und Obermiozän der Oberen Süßwassermolasse Süddeutschlands: Odontologie und Osteologie. Münchner Geowissenschaftliche Abhandlungen (A) 36, 1–245.
Gray, H., 1918. Anatomy of the Human Body. Lea & Febiger, Philadelphia, pp. 1–1364.
Harington, C., Mol, D., van der Plicht, J., 2012. The Muirkirk mammoth: a Late Pleistocene woolly mammoth (*Mammuthus primigenius*) skeleton from southern Ontario, Canada. Quaternary International 255, 106–113.
Hautier, L., Stansfield, F.J., Allen, W.T., Asher, R.J., 2012. Skeletal development in the African elephant and ossification timing in placental mammals. Proceedings of the Royal Society B: Biological Sciences 279, 2188–2195.
Haynes, G., 1991. Mammoths, Mastodonts, and Elephants: Biology, Behavior and the Fossil Record. Cambridge University Press, New york, pp. 1–354.
Hou, Y.M., Zhao, L.X., 2010. An archeological view for the presence of early humans in China. Quaternary International 223, 10–19.
Keates, S.G., 2010. Evidence for the earliest Pleistocene hominid activity in the Nihewan Basin of northern China. Quaternary International 223, 408–417.
Laws, R., 1966. Age criteria for the African elephant. African Journal of Ecology 4 (1), 1–37.
Lister, A.M., 1993. 'Gradualistic'evolution: its interpretation in Quaternary large mammal species. Quaternary International 19, 77–84.
Lister, A.M., 1996. Evolution and taxonomy of Eurasian mammoths. In: Shoshani, J., Tassy, P. (Eds.), The Proboscidea: Evolution and Paleoecology of Elephants and Their Relatives. Oxford University Press, New York, pp. 203–213.
Lister, A., 1999. Epiphyseal fusion and postcranial age determination in the woolly mammoth, *Mammuthus primigenius* (Blum.). Deinsea 6, 79–88.
Lister, A.M., Sher, A.V., van Essen, H., Wei, G., 2005. The pattern and process of mammoth evolution in Eurasia. Quaternary International 126, 49–64.
Lister, A.M., Stuart, A.J., 2010. The West Runton mammoth (*Mammuthus trogontherii*) and its evolutionary significance. Quaternary International 228 (1), 180–209.
Lister, A.M., Dimitrijević, V., Marković, Z., Knežević, S., Mol, D., 2012. A skeleton of 'steppe'mammoth (*Mammuthus trogontherii* (Pohlig)) from Drmno, near Kostolac, Serbia. Quaternary International 276, 129–144.
Liu, P., Wu, Z., Deng, C., Tong, H., Qin, H., Li, S., Yuan, B., Zhu, R., 2016. Magnetostratigraphic dating of the Shanshenmiaozui mammalian fauna in the Nihewan Basin, North China. Quaternary International 400, 202–211.
Maschenko, E., 2002. Individual development, biology and evolution of the woolly mammoth. Cranium 19 (1), 1–120.
Maschenko, E., Tikhonov, A.N., MacPhee, R.D., 2005. Mammoth calf from Bolshoi Lyakhovskii island (New Siberian islands, Arctic Siberia). Russian Journal of Theriology 4 (1), 79–88.
Maschenko, E., Schvyreva, A.K., Kalmykov, N., 2011. The second complete skeleton of *Archidiskodon meridionalis* (Elephantidae, Proboscidea) from the Stavropol region, Russia. Quaternary Science Reviews 30 (17), 2273–2288.
Maschenko, E., Boeskorov, G., Baranov, V., 2013a. Morphology of a mammoth calf (*Mammuthus primigenius*) from Ol'chan (Oimiakon, Yakutia). Paleontological Journal 47 (4), 425–438.
Maschenko, E., Protopopov, A., Plotnikov, V., Pavlov, I., 2013b. Specific characters of the mammoth calf (*Mammuthus primigenius*) from the Khroma river (Yakutia). Biology Bulletin 40 (7), 626–641.
Maschenko, E.N., 2006. New data on the morphology of a foetal mammoth (*Mammuthus primigenius*) from the Late Pleistocene of southwestern Siberia. Quaternary international 142, 130–146.
Miller, C., Basu, C., Fritsch, G., Hildebrandt, T., Hutchinson, J., 2008. Ontogenetic scaling of foot musculoskeletal anatomy in elephants. Journal of the Royal Society Interface 5 (21), 465–475.
Peterson, H.A., 2007. Epiphyseal Growth Plate Fractures. Springer, Heidelberg, pp. 1–914.
Popescu, A., 2011. The tarsals of *Mammuthus meridionalis* (NESTI, 1825) from Leu (Dolj County, Romania). GeoEcoMarina 17, 211–217.
Roth, V., Shoshani, J., 1988. Dental identification and age determination in *Elephas maximus*. Journal of Zoology 214 (4), 567–588.
Roth, V.L., 1984. How elephants grow: heterochrony and the calibration of developmental stages in some living and fossil species. Journal of Vertebrate Paleontology 4 (1), 126–145.
Siegal-Willott, J., Isaza, R., Johnson, R., Blaik, M., 2008. Distal limb radiography, ossification, and growth plate closure in the juvenile Asian elephant (*Elephas maximus*). Journal of Zoo and Wildlife Medicine 39 (3), 320–334.
Sikes, S.K., 1971. Natural History of the African Elephant. Weidenfeld and Nicolson, London, pp. 1–379.
Silver, I., 1969. The ageing of domestic animals. In: Brothwell, D.R., Higgs, E.S. (Eds.), Science and Archaeology. A Survey of Progress and Research. Thames and Hudson, London, pp. 250–268.
Teilhard de Chardin, P., 1936. Fossil mammals from locality 9 of Choukoutien. Palaeontologia Sinica, Series C VII (Fasc.4), 1–61.
Tong, H.-W., 2012. New remains of *Mammuthus trogontherii* from the early Pleistocene Nihewan beds at Shanshenmiaozui, Hebei. Quaternary International 255, 217–230.
Tong, H.-W., Chen, X., 2016. On newborn calf skulls of early Pleistocene *Mammuthus trogontherii* from Shanshenmiaozui in Nihewan Basin, China. Quaternary International 406, 57–69.
Tong, H., Hu, N., Han, F., 2011. A preliminary report on the excavations at the early Pleistocene fossil site of Shanshenmiaozui in Nihewan Basin, Hebei, China. Quaternary Sciences 31 (4), 643–653.
Von den Driesch, A., 1976. A guide to the measurement of animal bones from archaeological sites: as developed by the Institut für Palaeoanatomie, Domestikationsforschung und Geschichte der Tiermedizin of the University of Munich. Peabody Museum Press, pp. 1–136.
Wei, G., Taruno, H., Jin, C., Xie, F., 2003. The earliest specimens of the steppe mammoth, *Mammuthus trogontherii*, from the early Pleistocene Nihewan formation, North China. Earth Science (Japan) 57 (5), 289–298.
Wei, G., Hu, S., Yu, K., Hou, Y., Li, X., Jin, C., Wang, Y., Zhao, J., Wang, W., 2010. New materials of the steppe mammoth, *Mammuthus trogontherii*, with discussion on the origin and evolutionary patterns of mammoths. Science China (Earth Sciences) 53 (7), 956–963.
Wei, G.B., Taruno, H., Kawamura, Y., Jin, C.Z., 2006. Pliocene and Early Pleistocene primitive mammoths of northern China: their revised taxonomy, biostratigraphy and evolution. Journal of Geosciences 49, 59–101. Osaka City University.
Zhu, R., Potts, R., Xie, F., Hoffman, K.A., Deng, C.L., Shi, C., Pan, Y.X., Wang, H., Shi, R., Wang, Y., 2004. New evidence on the earliest human presence at high northern latitudes in northeast Asia. Nature 431 (7008), 559–562.
Ziegler, R., 2001. An extraordinary small mammoth (*Mammuthus primigenius*) from SW Germany. Stuttgarter Beiträge zur Naturkunde Serie B (Geologie und Paläontologie) 300, 1–41.